Generation of dark solitons in erbium-doped fiber lasers based Sb_2Te_3 saturable absorbers

Wenjun Liu,[1,2] Lihui Pang, [2] Hainian Han, [2] Wenlong Tian, [2] Hao Chen, [3] Ming Lei, [1] Peiguang Yan,[3] and Zhiyi Wei[2,*]

[1] *State Key Laboratory of Information Photonics and Optical Communications, School of Science, P. O. Box 91, Beijing University of Posts and Telecommunications, Beijing 100876, China*

[2] *Beijing National Laboratory for Condensed Matter Physics, Institute of Physics, Chinese Academy of Sciences, Beijing 100190, China*

[3] *Shenzhen Key Laboratory of Laser Engineering, College of Optoelectronic Engineering, Shenzhen University, ShenZhen, 518060, China*

[*] *zywei@iphy.ac.cn*

Abstract: Dark solitons, which have better stability in the presence of noise, have potential applications in optical communication and ultrafast optics. In this paper, the dark soliton formation in erbium-doped fiber lasers based Sb_2Te_3 saturable absorber (SA) is first experimentally demonstrated. The Sb_2Te_3 SA is fabricated by using the pulsed laser deposition method. The generated dark solitons are centered at the wavelength of 1530 nm and repetition rate of 94 MHz. Analytic solutions for dark solitons are also obtained theoretically.

OCIS codes: (060.5530) Pulse propagation and temporal solitons; (140.3510) Lasers, fiber; (140.4050) Mode-locked lasers.

References and links

1. R. K. Dodd, J. C. Eilbeck, J. D. Gibbon, and H. C. Morris, *Solitons and Nonlinear Wave Equations* (Academic Press, 1982).
2. N. P. Proukakis, N. G. Parker, D. J. Frantzeskakis, and C. S. Adams, "Analogies between dark solitons in atomic Bose-Einstein condensates and optical systems," J. Opt. B Quantum Semiclassical Opt. **6**(5), S380–S391 (2004).
3. D. J. Frantzeskakis, "Dark solitons in atomic Bose-Einstein condensates: from theory to experiments," J. Phys. A Math. Theor. **43**(21), 213001 (2010).
4. Y. S. Kivshar and B. Luther-Davies, "Dark optical solitons: Physics and applications," Phys. Rep. **298**(2-3), 81–197 (1998).
5. P. Emplit, J. P. Hamaide, R. Reynaud, C. Froehly, and A. Barthelemy, "Picosecond steps and dark pulses through nonlinear single mode fibers," Opt. Commun. **62**(6), 374–379 (1987).
6. Y. F. Song, J. Guo, L. M. Zhao, D. Y. Shen, and D. Y. Tang, "280 GHz dark soliton fiber laser," Opt. Lett. **39**(12), 3484–3487 (2014).
7. W. Zhao and E. Bourkoff, "Generation, propagation, and amplification of dark solitons," J. Opt. Soc. Am. B **9**(7), 1134–1144 (1992).
8. G. P. Agrawal, Nonlinear Fiber Optics, 3rd ed., Academic press, San Diego (2002).
9. W. Zhao and E. Bourkoff, "Propagation properties of dark solitons," Opt. Lett. **14**(13), 703–705 (1989).
10. Y. S. Kivishar and G. Agrawal, Optical Solitons: From Fiber to Photonic Crystals, Academic, New York, NY, USA, 2003.
11. B. A. Malomed, A. Mostofi, and P. L. Chu, "Transformation of a dark soliton into a bright pulse," J. Opt. Soc. Am. B **17**(4), 507–513 (2000).
12. H. Zhang, D. Y. Tang, L. M. Zhao, and R. J. Knize, "Vector dark domain wall solitons in a fiber ring laser," Opt. Express **18**(5), 4428–4433 (2010).
13. Y. S. Kivshar, M. Haelterman, P. Emplit, and J. P. Hamaide, "Gordon-Haus effect on dark solitons," Opt. Lett. **19**(1), 19–21 (1994).
14. H. Zhang, D. Y. Tang, L. M. Zhao, and X. Wu, "Dark pulse emission of a fiber laser," Phys. Rev. A **80**(4), 045803 (2009).
15. M. Feng, K. L. Silverman, R. P. Mirin, and S. T. Cundiff, "Dark pulse quantum dot diode laser," Opt. Express **18**(13), 13385–13395 (2010).
16. D. Y. Tang, L. Li, Y. F. Song, L. M. Zhao, H. Zhang, and D. Y. Shen, "Evidence of dark solitons in all-normal-dispersion-fiber lasers," Phys. Rev. A **88**(1), 013849 (2013).
17. D. Tang, J. Guo, Y. Song, H. Zhang, L. Zhao, and D. Shen, "Dark soliton fiber lasers," Opt. Express **22**(16), 19831–19837 (2014).
18. Y. Q. Ge, J. L. Luo, L. Li, X. X. Jin, D. Y. Tang, D. Y. Shen, S. M. Zhang, and L. M. Zhao, "Initial conditions for dark soliton generation in normal-dispersion fiber lasers," Appl. Opt. **54**(1), 71–75 (2015).

#247774 Received 13 Aug 2015; revised 16 Sep 2015; accepted 20 Sep 2015; published 24 Sep 2015

19. T. Sylvestre, S. Coen, P. Emplit, and M. Haelterman, "Self-induced modulational instability laser revisited: normal dispersion and dark-pulse train generation," Opt. Lett. **27**(7), 482–484 (2002).
20. H. S. Yin, W. C. Xu, A. P. Luo, Z. C. Luo, and J. R. Liu, "Observation of dark pulse in a dispersion-managed fiber ring laser," Opt. Commun. **283**(21), 4338–4341 (2010).
21. I. N. Iii, "All-fiber ring soliton laser mode locked with a nonlinear mirror," Opt. Lett. **16**(8), 539–541 (1991).
22. V. J. Matsas, T. P. Newson, D. J. Richardson, and D. J. Payne, "Selfstarting passively mode-locked fibre ring soliton laser exploiting nonlinear polarisation rotation," Electron. Lett. **28**(15), 1391–1393 (1992).
23. H. Zhang, D. Y. Tang, X. Wu, and L. M. Zhao, "Multi-wavelength dissipative soliton operation of an erbium-doped fiber laser," Opt. Express **17**(15), 12692–12697 (2009).
24. Z. Luo, A. Luo, and W. Xu, "Tunable and switchable multiwavelength passively mode-locked fiber laser based on SESAM and inline birefringence comb filter," IEEE Photonics J. **3**(1), 64–70 (2011).
25. X. Zhao, Z. Zheng, L. Liu, Y. Liu, Y. Jiang, X. Yang, and J. Zhu, "Switchable, dual-wavelength passively mode-locked ultrafast fiber laser based on a single-wall carbon nanotube modelocker and intracavity loss tuning," Opt. Express **19**(2), 1168–1173 (2011).
26. X. Li, Y. Wang, Y. Wang, X. Hu, W. Zhao, X. Liu, J. Yu, C. Gao, W. Zhang, and Z. Yang, "Wavelengthswitchable and wavelength-tunable all-normal-dispersion mode-locked Yb-doped fiber laser based on singlewalled carbon nanotube wall paper absorber," IEEE Photonics J. **4**(1), 234–241 (2012).
27. H. Zhang, D. Y. Tang, R. J. Knize, L. M. Zhao, Q. L. Bao, and K. P. Loh, "Graphene mode locked, wavelength-tunable, dissipative soliton fiber laser," Appl. Phys. Lett. **96**(11), 111112 (2010).
28. S. Huang, Y. Wang, P. Yan, J. Zhao, H. Li, and R. Lin, "Tunable and switchable multi-wavelength dissipative soliton generation in a graphene oxide mode-locked Yb-doped fiber laser," Opt. Express **22**(10), 11417–11426 (2014).
29. C. Zhao, Y. Zou, Y. Chen, Z. Wang, S. Lu, H. Zhang, S. Wen, and D. Tang, "Wavelength-tunable picosecond soliton fiber laser with Topological Insulator: Bi_2Se_3 as a mode locker," Opt. Express **20**(25), 27888–27895 (2012).
30. P. Yan, R. Lin, H. Chen, H. Zhang, A. Liu, H. Yang, and S. Ruan, "Topological insulator solution filled in photonic crystal fiber for passive mode-locked fiberlaser," IEEE Photonics Technol. Lett. **27**(3), 264–267 (2015).
31. P. Yan, R. Lin, S. Ruan, A. Liu, and H. Chen, "A 2.95 GHz, femtosecond passive harmonic mode-locked fiber laser based on evanescent field interaction with topological insulator film," Opt. Express **23**(1), 154–164 (2015).
32. L. M. Zhao, D. Y. Tang, H. Zhang, X. Wu, Q. Bao, and K. P. Loh, "Dissipative soliton operation of an ytterbium-doped fiber laser mode locked with atomic multilayer graphene," Opt. Lett. **35**(21), 3622–3624 (2010).
33. J. Xu, S. Wu, H. Li, J. Liu, R. Sun, F. Tan, Q. H. Yang, and P. Wang, "Dissipative soliton generation from a graphene oxide mode-locked Er-doped fiber laser," Opt. Express **20**(21), 23653–23658 (2012).
34. Y. F. Song, L. Li, H. Zhang, Y. Shen, D. Y. Tang, and K. P. Loh, "Vector multi-soliton operation and interaction in a graphene mode-locked fiber laser," Opt. Express **21**(8), 10010–10018 (2013).
35. S. Lu, C. Zhao, Y. Zou, S. Chen, Y. Chen, Y. Li, H. Zhang, S. Wen, and D. Tang, "Third order nonlinear optical property of Bi_2Se_3," Opt. Express **21**(2), 2072–2082 (2013).
36. J. Wang, Z. Cai, P. Xu, G. Du, F. Wang, S. Ruan, Z. Sun, and T. Hasan, "Pulse dynamics in carbon nanotube mode-locked fiber lasers near zero cavity dispersion," Opt. Express **23**(8), 9947–9958 (2015).
37. P. Wong, W. J. Liu, L. G. Huang, Y. Q. Li, N. Pan, and M. Lei, "Higher-order-effects management of soliton interactions in the Hirota equation," Phys. Rev. E Stat. Nonlin. Soft Matter Phys. **91**(3), 033201 (2015).
38. W. Liu, B. Tian, H. Zhang, T. Xu, and H. Li, "Solitary wave pulses in optical fibers with normal dispersion and higher-order effects," Phys. Rev. A **79**(6), 063810 (2009).
39. R. Hirota, "Exact solution of the Korteweg-de Vries equation for multiple collisions of solitons," Phys. Rev. Lett. **27**(18), 1192–1194 (1971).

1. Introduction

Solitons, which can be divided into bright and dark ones, exist in nonlinear systems [1]. If the effective nonlinearity in systems is attractive, then bright solitons are formed, while dark solitons appear in the opposite case [2]. Dark solitons have the form of a density dip with a phase jump across its density minimum. And this kind of localized nonlinear waves exists on the top of a stable continuous wave background [3].

In the past decades, dark solitons are widely applied in nonlinear optics and ultra-fast optics, and the formation of them in mode-locked fiber lasers has been studied because of their applications [4]. Like the formation of bright solitons, dark soliton formation is an intrinsic feature of the nonlinear light propagation in the normal dispersion regimes [5, 6]. Compared to bright solitons, dark solitons have the advantages of having better stability in the presence of noise and being less influenced by intrapulse-stimulated Raman scattering [7–9]. Besides, dark solitons have been broadened during the propagation at nearly half the rate of bright solitons. Those advantages enable dark solitons to be more suitable than bright solitons in nonlinear optics [10–13].

#247774 Received 13 Aug 2015; revised 16 Sep 2015; accepted 20 Sep 2015; published 24 Sep 2015

Dark soliton generation in erbium-doped fiber (EDF) lasers of normal dispersion has been first observed in [14], awaking research interests for exploring new sources for the dark soliton generation [15]. Different from fibers, the existence of a gain-loss mechanism, gain dispersion effect, and the cavity boundary condition in fiber lasers should be taken into account for the dark soliton generation. As a result, dark solitons can be generated in fiber lasers only for certain parameters [14,16,17]. Thus, meaningful work that testing different initial conditions on fiber lasers with selected cavity parameters and operation conditions has been done [18–20].

On the other hand, to achieve passive mode locking of a fiber laser, different techniques have been used. These conventional techniques include the figure-of-eight cavity method and nonlinear polarization rotation (NPR) technique [21,22]. Due to their disadvantages and drawbacks, the real and novel saturable absorbers (SAs) such as the semiconductor saturable absorber mirrors (SESAM) [23,24], single wall carbon nanotubes [25,26], graphene [27,28] as well as topological insulators (TIs) [29–31] have been applied to achieve passive mode-locking and realize soliton operations. Tunable dissipative soliton generation, as well as vector multi-soliton operation and interaction in graphene oxide mode-locked fiber laser, have been investigated experimentally [32–34]. Unlike grapheme, TIs, such as Bi_2Te_3, Bi_2Se_3 and Sb_2Te_3, have the characteristics with a small band gap in the bulk state and a gapless metallic state in the surface. They have broadband saturable absorption features and giant third order nonlinear optical property [30,31]. Based on the Bi_2Se_3 SA, the stable soliton pulses with 1.57 ps was first observed in an EDF laser [29]. Regrettably is that there are few reports on dark solitons in EDF lasers with Sb_2Te_3 SA in the existing literature.

In this paper, dark solitons in EDF lasers based Sb_2Te_3 SA will be obtained for the first time to our knowledge. In order to controlling the length of a deposited material, layers of Sb_2Te_3 will be deposited on a microfiber, which enables the interaction between the evanescent fields. The Sb_2Te_3 SAs will be fabricated with the pulsed laser deposition (PLD) method. Combining the NPR technique, the EDF lasers based Sb_2Te_3 SAs will be mode locked. The optical spectrum of dark solitons will be centered at 1530 nm. The output power of dark solitons will be 12 mW. The formation of dark solitons in the proposed fiber lasers will also be studied analytically. The analytic dark soliton solutions for the nonlinear Schrödinger (NLS) equation, which can describe the formation of dark solitons in such fiber lasers, will be derived. Agreement between experimental and analytical results will be discussed.

2. Fabriation and characterization of Sb_2Te_3 SA

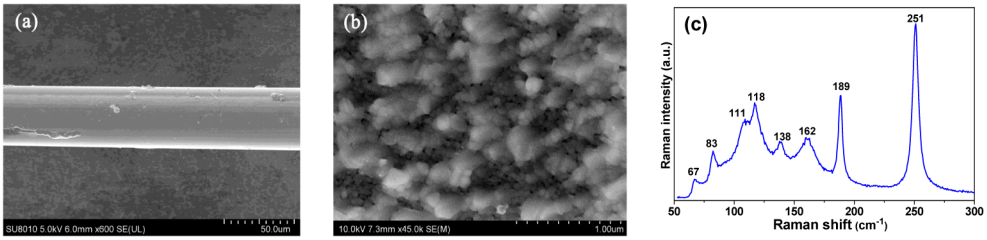

Fig. 1. Characterization of a prepared Sb_2Te_3 layer: (a) SEM images of fiber taper, (b) enlarged film surface, (c) Raman spectrum.

The fabrication process is divided into two steps: fused-tapering and PLD coating. At first, the SMF-28 fiber is tapered to microfiber. Generally, the waist diameter of the fiber can be tapered down from a few micrometers to tens of micrometers. In this paper, the tapered waist of microfiber has the length of 2 mm, and the diameter is about 18 μm. And then, a high energy Nd:YAG laser (SL II-10, Surelite, λ = 1550 nm) is operated with 200 mJ/pulse (2 W average power, and 10 Hz repetition rate). With vacuum degree of 10^{-4} pa, the laser beam is focused on the Sb_2Te_3 target inside a vacuum chamber. The inspired plasma plume is

#247774 Received 13 Aug 2015; revised 16 Sep 2015; accepted 20 Sep 2015; published 24 Sep 2015

deposited on microfiber within 60 minutes. To avoid pollution from the plastic polymers of the fiber, the deposition temperature is fixed at room temperature. Figure 1(a) is the scanning electron microscope (SEM) images of the tapered waist of microfiber, and Fig. 1(b) is one part of the enlarged regions of Sb_2Te_3 film. The nonlinear effect of the Sb_2Te_3 SA can be adjusted by depositing Sb_2Te_3 onto the microfiber, where the deposited amount and length of Sb_2Te_3 along the microfiber are able to be controlled by adjusting the deposition time. Hence, it can increase the interaction between propagating beam and Sb_2Te_3. By using a Raman spectrometer (LabRAM HR Evolution) with a laser at 514 nm, Raman spectra is measured as shown in Fig. 1(c). To excite the Raman scatting, a typical laser power of 5.6 mW is used. The lines observed at 66, 111, and 162 cm^{-1} are well related to A_{1g} and E_g modes of Sb_2Te_3. The lines at 189 and 251 cm^{-1} are related to Sb_2O_3.

The insertion loss (IL) of the Sb_2Te_3 SA is measured to be ~2 dB. The input amplified spontaneous emission (ASE) light source (Glight, 1250 nm~1650 nm) and optical spectrum analyzer (Yokogawa AQ6315A) are used to measure the device's linear absorption from 1400 nm to 1600 nm. The linear transmission is characterized by a very flat profile at the level of 65% ± 2% in Fig. 2(a). Using a femtosecond pulse with pulse duration of 650 fs, central wavelength of 1562 nm, and repetition rate of 22.5 MHz, the nonlinear saturable absorption is measured as shown in Fig. 2(b). The saturable intensity is 175 MW/cm^2, and a modulation depth $\Delta\alpha$ is about 7.42%.

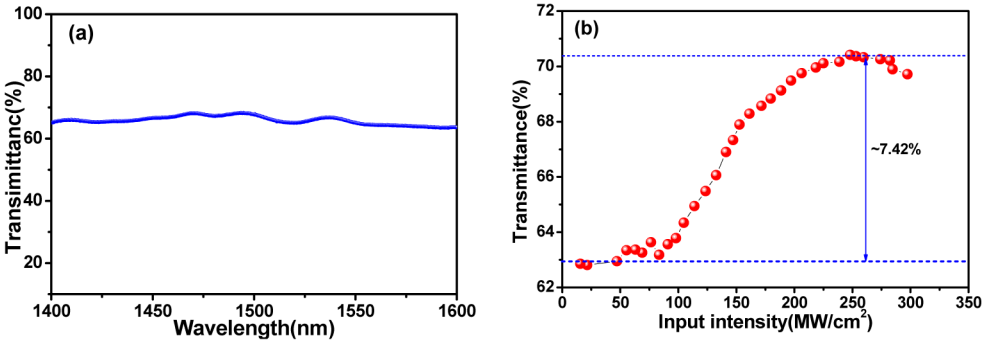

Fig. 2. (a) Measured linear absorption, (b) measured nonlinear saturable absorption of the fiber-taper TI: Sb_2Te_3 SA.

3. Mode-locked EDF laser setup

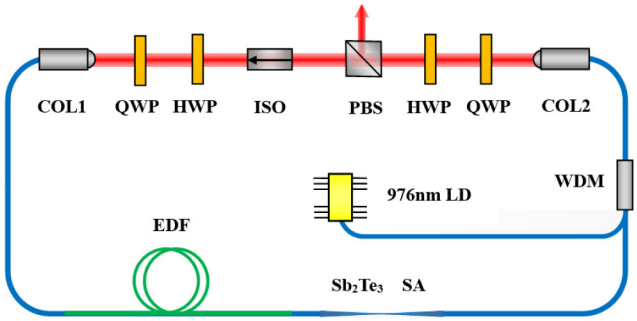

Fig. 3. Configuration of the mode-locked EDF laser. COL, collimator; QWP, quarter waveplate; HWP, half waveplate; ISO, polarization-dependent isolator; PBS, polarization beam splitter; WDM, wavelength-division multiplexer.

Figure 3 shows the schematic of mode-locked EDF laser with our Sb_2Te_3 SA device. The pump source is a laser diode (LD) with emission centered at 976 nm with maximum output

#247774 Received 13 Aug 2015; revised 16 Sep 2015; accepted 20 Sep 2015; published 24 Sep 2015

power of 500 mW. A 370-mm-long EDF (Liekki 110 −4/125) is used as the gain medium with absorption coefficient of 110 dB/m at 1530 nm. The QWP and HWP are employed to adjust the polarization state of pulses. Unidirectional operation of the fiber laser is ensured by the ISO. The pump is delivered into EDF via a 980/1550 nm wavelength division multiplexer (WDM) with two HI1060 fiber pigtail. The leading fiber of collimators is the SMF-28 fiber. The Sb_2Te_3 SA is inserted between the EDF and WDM. The total cavity length is about 2.2 m. Because our Sb_2Te_3 SA device is a hybrid structure composed by the inner microfiber and the outer coated thin TI film, the dispersion of which could not be accurately valued, the total cavity dispersion is difficult to be determined. An optical spectrum analyzer (Yokogawa AQ6315A) and a 250-MHz oscilloscope (Tektronix TDS 714L) with a 1-GHz photo-detector are used to study the optical spectrum and output pulse train from the intra-cavity PBS, respectively.

4. Experimental results and discussions

In the experiment, the mode-locking threshold is about 120 mW. The output power of the mode-locked EDF laser is about 12 mW with the pump power of 350 mW. When the pump power is between 120 and 400 mW, the mode-locked EDF laser could maintain the mode-locking state without rotating the QWP and HWP in the ring cavity. As the increasing of the pump power, the output spectrum is broadened. The optical spectrum of mode-locked pulses is centered at 1530 nm in Fig. 4(a). The oscilloscope trace of dark solitons in the time scales of 10 ns/div can be seen in Fig. 4(b). Dark solitons emitted from the intra-cavity PBS with the repetition rate of 94 MHz, which is measured by a radio frequency analyzer (Agilent E4407B). The electrical signal to noise ratio (SNR) of the fundamental frequency is about 63 dB measured with 10 kHz resolution bandwidth, which indicates robust mode-locking as shown in Fig. 4(c). When we reduce the length of SMF-28 fiber (about 80mm) in the mode-locked EDF laser, and rotate the QWP and HWP in the ring cavity to change the intra-cavity polarization, bright solitons can be observed. However, we only focuse on dark soliton operation in this paper. Thus, the total cavity dispersion of the mode-locked EDF laser has important effect on the generation of dark solitons. Finally, we remove the Sb_2Te_3 SA, dark solitons cannot be observed no matter how we adjust the pump power and rotate the QWP and HWP. Because Sb_2Te_3 SA shows a giant nonlinear refreactive index, and can induce the high nonlinear effect [35], dark solitons can be generated when the EDF laser is mode locked based on the Sb_2Te_3 SA. Finally, our Sb_2Te_3 SA device fabricated with the PLD method is demonstrated to be the good candidates of highly nonlinear photonic device in fiber lasers. We hope better results on dark solitons in our fiber lasers could be presented in the future research.

#247774 Received 13 Aug 2015; revised 16 Sep 2015; accepted 20 Sep 2015; published 24 Sep 2015

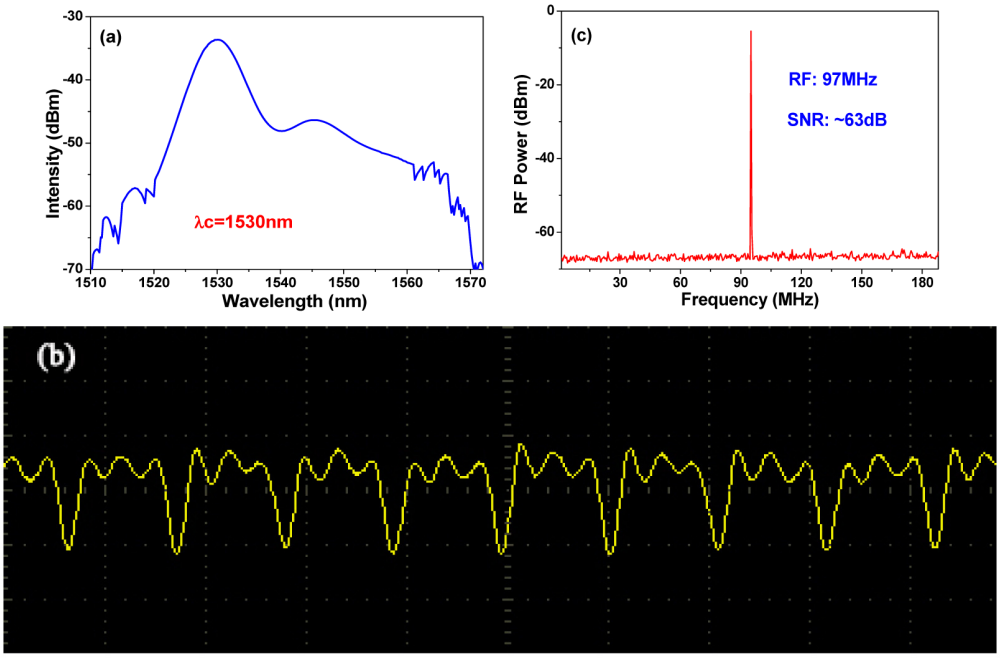

Fig. 4. Experimental results of the mode-locked EDF laser: (a) Optical spectrum of dark solitons, (b) the oscilloscope trace of dark solitons in the time scales of 10 ns/div, (c) radio frequency (RF) spectrum of the mode-locked laser.

5. Analytic study on dark solitons

The mode-locked EDF laser based Sb_2Te_3 SA can be modeled by the nonlinear Schrödinger (NLS) equation as follows [36],

$$\frac{\partial A}{\partial z} = -i\frac{\beta_2(z)}{2}\frac{\partial^2 A}{\partial \tau^2} + i\gamma(z)|A|^2 A + \frac{g(z)}{2}A, \tag{1}$$

where $A(z,\tau)$ represents the optical field amplitude, z is the propagation distance, and τ is the retarded time in the model of soliton fiber lasers. $\beta_2(z)$ is the group-velocity dispersion (GVD), $\gamma(z)$ is the nonlinear effect, and $g(z)$ is the linear gain. By introducing the dependent variable transformation [37,38]:

$$A(z,\tau) = \frac{g(z,\tau)}{f(z,\tau)}, \tag{2}$$

where $g(z,\tau)$ is a complex differentiable function, and $f(z,\tau)$ is a real one. For simplicity, $g(z,\tau)$ and $f(z,\tau)$ are replaced with g and f, respectively. After some symbolic manipulations, we can obtain the bilinear form for Eq. (1) as

$$[D_z + \frac{i}{2}\beta_2(z)D_\tau^2 - \lambda(z)]g\bullet f = 0, \tag{3}$$

$$[\frac{i}{2}\beta_2(z)D_\tau^2 - \lambda(z)]f\bullet f = -i\exp[\int g(z)dz]\gamma(z)|g|^2. \tag{4}$$

#247774 Received 13 Aug 2015; revised 16 Sep 2015; accepted 20 Sep 2015; published 24 Sep 2015

Here, $\lambda(z)$ is a function to be determined and the Hirota bilinear operators D_z and D_τ are defined by [39]

$$D_z^m D_\tau^n (g\cdot f) = (\frac{\partial}{\partial x}-\frac{\partial}{\partial x'})^m (\frac{\partial}{\partial t}-\frac{\partial}{\partial t'})^n \times g(x,t)f(x',t')\,|_{x'=x,t'=t}\ .$$

Bilinear forms (3) and (4) can be solved by the following power series expansions for g and f

$$g = g_0(1+\varepsilon g_1+\varepsilon^2 g_2+\cdots), \tag{5}$$

$$f = 1+\varepsilon f_1+\varepsilon^2 f_2+\cdots, \tag{6}$$

where ε is a formal expansion parameter. Substituting expressions (5) and (6) into bilinear forms (3) and (4), and equating coefficients of the same powers of ε to zero yield the recursion relations for $g_n's$ and $f_n's$. Then, analytic solutions for Eq. (1) can be obtained.

For the analytic soliton solution of Eq. (1), g_0, g_1 and f_1 are assumed to be in the following form:

$$g_0 = m\exp[ik_1(z)+i\omega_1\tau],\quad g_1 = n\exp[k_2(z)+\omega_2\tau+\sigma],\quad f_1 = \rho(z)\exp[k_2(z)+\omega_2\tau+\sigma],$$

with $k_j(z),(j=1,2)$ are differentiable functions of z to be determined, and m, n, σ and ω_j are real constants. Substituting g_0, g_1 and f_1 into the resulting set of linear partial differential equations which refer to the above recursion relations yielded by equating coefficients of the same powers of ε to zero and after some calculations, we can get the constraints on the parameters:

$$\lambda(z) = i|m|^2\exp[\int g(z)dz]\gamma(z),\qquad \beta_2(z) = \frac{4|m|^2\exp[\int g(z)dz]\gamma(z)}{\omega_2{}^2},$$

$$k_2(z) = \frac{\omega_1}{\omega_2}\int 4|m|^2\exp[\int g(z)dz]\gamma(z)]dz,\quad \rho(z) = \frac{2n|m|^2\exp[\int g(z)dz]\gamma(z)}{2|m|^2\exp[\int g(z)dz]\gamma(z)-\omega_2{}^2\beta_2(z)},$$

$$k_1(z) = \int[\frac{1}{2}\omega_1{}^2\beta_2(z)+|m|^2\exp[\int g(z)dz]\gamma(z)]dz$$

and $g_n = 0,\ f_n = 0$ ($n = 2,3,4,\ldots\ldots$).

Without loss of generality, we set $\varepsilon = 1$, thus, the analytic dark soliton solution for Eq. (1) can be obtained as

$$A(z,\tau) = \frac{g}{f} = \frac{g_0(1+g_1)}{1+f_1} = m\exp[i\omega_1 t+\frac{1}{2}\int g(z)dz+\int\lambda(z)dz+\frac{i\omega_1}{2\omega_2}\int k_2(z)dz]\mathrm{Tanh}[k_2(z)+\omega_2\tau+\sigma]. \tag{7}$$

According to solution (7), we select a series of physical parameters as $g(z) = 0.000892dB/m$, $\gamma(z) = 0.0023W^{-1}m^{-1}$ and $\beta_2(z)\approx 2.3fs^2mm^{-1}$. The free parameters are choosen as $m=1$, $n=-1$, $\omega_1=1$, $\omega_2=2$ and $\sigma=-5.3$. Fig. 5 shows the simulated dark soliton formation with analytic solution (7). The transmission of dark solitons is stable with those parameters relationship. In Fig. 5(b), we choose the nonlinear coefficient $\gamma(z)$ as the

#247774 Received 13 Aug 2015; revised 16 Sep 2015; accepted 20 Sep 2015; published 24 Sep 2015

Gaussian function, such as $\gamma(z) = 0.0023\exp(-2x^2)$, which means that the nonlinearity of the EDF laser changes in the form of Gauss profile. With the constraint $\beta_2(z) = 4|m|^2 \exp[\int g(z)dz]\gamma(z)/\omega_2^2$, the GVD coefficient $\beta_2(z)$ is equal to $2.3\exp(0.000892x - 2x^2)$. In that case, dark solitons are also generated. In addition, if we change the values of $g(z)$, $\gamma(z)$ and $\beta_2(z)$, the pulse duration and pulse intensity can be adjusted. When the pump power is determined, the pulse intensity is related to $m\exp[\frac{1}{2}\int g(z)dz]$, which means that $g(z)$ has the mainly impact on the pulse intensity although $\gamma(z)$ and $\beta_2(z)$ have some influnces on it. The pulse duration is determined by $\gamma(z)$ and $\beta_2(z)$.

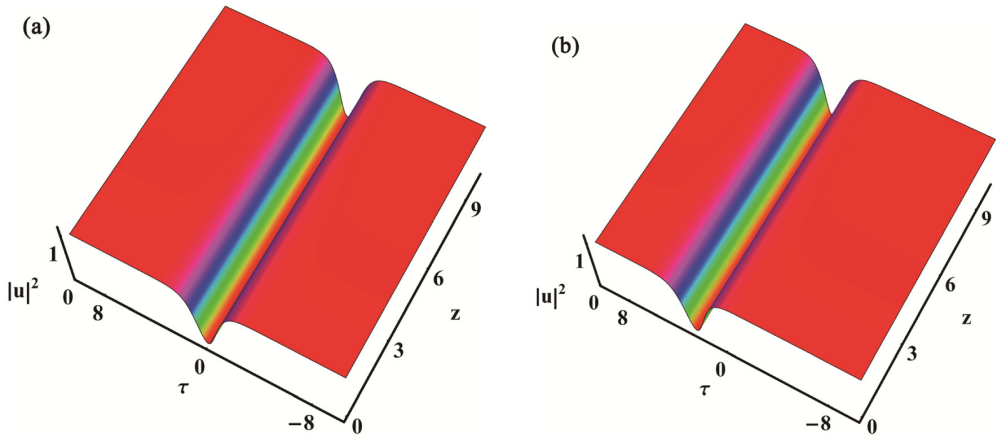

Fig. 5. Analytically simulated dark soliton formation with solution (7) in Eq. (1). The corresponding parameters are $g(z) = 0.000892dB/m$, $m = 1$, $n = -1$, $\omega_1 = 1$, $\omega_2 = 2$ and $\sigma = -5.3$ with (a) $\gamma(z) = 0.0023W^{-1}m^{-1}$, $\beta_2(z) \approx 2.3fs^2mm^{-1}$, (b) $\gamma(z) = 0.0023\exp(-2x^2)$ and $\beta_2(z) \approx 2.3\exp(0.000892x - 2x^2)$.

6. Conclusion

The generation of dark solitons in EDF lasers based Sb_2Te_3 SA has been presented in this paper, for the first time to our best knowledge. With the PLD method, the Sb_2Te_3 SA has been fabricated. Using an evanescent field interaction with the Sb2Te3 TI, the EDF laser can be operated in the mode locking state. Dark solitons have been formed at 1530nm with a frequency of 94 MHz. Moreover, analytic solutions for dark solitons have been obtained theoretically, and the influences of $g(z)$, $\gamma(z)$ and $\beta_2(z)$ have been discussed. The proposed Sb_2Te_3 SA device fabricated with the PLD method has been demonstrated to be the good candidates of highly nonlinear photonic device in fiber lasers. We belive that Sb_2Te_3 SA device could also be used in other fiber lasers to find important applications in the fields of nonlinear and ultrafast photonics in the future research.

Acknowledgments

We express our sincere thanks to the Editors and Referees for their valuable comments. This work has been supported by the National Key Basic Research Program of China (grant Nos. 2012CB821304 and 2013CB922402), by the National Natural Science Foundation of China (NSFC) (grant Nos. 61205064, 61378040 and 11078022), by the Fund of State Key

Laboratory of Information Photonics and Optical Communications (Beijing University of Posts and Telecommunications, grant No. 600100161).

#247774 Received 13 Aug 2015; revised 16 Sep 2015; accepted 20 Sep 2015; published 24 Sep 2015